SANDIA REPORT
SAND2009-6451
Unlimited Release
Printed October 2009

Microbial Agent Detection using Near-IR Electrophoretic and Spectral Signatures (MADNESS) for Rapid Identification in Detect-to-Warn Applications

Julia A. Fruetel, Anthony L. Gomez, Ray P. Bambha, Victoria A. VanderNoot, Karen Krafcik, Ronald F. Renzi

Prepared by
Sandia National Laboratories
Albuquerque, New Mexico 87185 and Livermore, California 94550

Sandia is a multiprogram laboratory operated by Sandia Corporation,
a Lockheed Martin Company, for the United States Department of Energy's
National Nuclear Security Administration under Contract DE-AC04-94AL85000.

Issued by Sandia National Laboratories, operated for the United States Department of Energy by Sandia Corporation.

Available to DOE and DOE contractors from
U.S. Department of Energy
Office of Scientific and Technical Information
P.O. Box 62
Oak Ridge, TN 37831

Telephone: (865) 576-8401
Facsimile: (865) 576-5728
E-Mail: reports@adonis.osti.gov
Online ordering: http://www.osti.gov/bridge

Available to the public from
U.S. Department of Commerce
National Technical Information Service
5285 Port Royal Rd.
Springfield, VA 22161

Telephone: (800) 553-6847
Facsimile: (703) 605-6900
E-Mail: orders@ntis.fedworld.gov
Online order: http://www.ntis.gov/help/ordermethods.asp?loc=7-4-0#online

SAND2009-6451
Unlimited Release
Printed October 2009

Microbial Agent Detection using Near-IR Electrophoretic and Spectral Signatures (MADNESS) for Rapid Identification in Detect-to-Warn Applications

Julia A. Fruetel, Anthony L. Gomez, Ray P. Bambha, Victoria A. VanderNoot, Karen Krafcik, Ronald F. Renzi
Sandia National Laboratories
P.O. Box 969
Livermore, CA 94550-0969

Abstract

Rapid identification of aerosolized biological agents following an alarm by particle triggering systems is needed to enable response actions that save lives and protect assets. Rapid identifiers must achieve species level specificity, as this is required to distinguish disease-causing organisms (e.g., *Bacillus anthracis*) from benign neighbors (e.g., *Bacillus subtilis*). We have developed a rapid (1-5 minute), novel identification methodology that sorts intact organisms from each other and particulates using capillary electrophoresis (CE), and detects using near-infrared (NIR) absorbance and scattering. We have successfully demonstrated CE resolution of *Bacillus* spores and vegetative bacteria at the species level. To achieve sufficient sensitivity for detection needs (~10^4 cfu/mL for bacteria), we have developed fiber-coupled cavity-enhanced absorbance techniques. Using this method, we have demonstrated ~two orders of magnitude greater sensitivity than published results for absorbing dyes, and single particle (spore) detection through primarily scattering effects. Results of the integrated CE-NIR system for spore detection are presented.

ACKNOWLEDGMENTS

The authors would like to thank Pam Lane and Julie Kaiser for growing up cells and generating spores for use in this project. This project was funded by LDRD. Sandia is a multiprogram laboratory operated by Sandia Corporation, a Lockheed Martin Company, for the United States Department of Energy's National Nuclear Security Administration under contract DE-AC04-94AL85000.

CONTENTS

FIGURES

TABLES

NOMENCLATURE

AOM	Acoustic optical modulator
CE	Capillary electrophoresis
CRDS	Cavity ring down spectroscopy
DOE	Department of Energy
IBB-CEAS	Incoherent broad band cavity enhanced absorption spectroscopy
GRIN	Graded index
kD	Kilodalton (1000 g/mol)
LOD	Limit of detection
MDAL	Minimum detectable absorption loss
MW	Molecular weight
NIR	Near infra-red
PEO	Polyethylene oxide
SNL	Sandia National Laboratories

INTRODUCTION

Rapid identifiers of aerosolized biological agents are desired by both DHS and DoD to rapidly (1-5 minutes) provide additional information following an alarm by aerosol particle triggering systems. Because particle triggering systems such as BAWS (DoD's Biological Agent Warning System) false alarm frequently on non-biological particles and cannot discriminate between pathogenic and non-pathogenic biological particles, rapid identification of the source of the trigger alarm is critical to enabling rapid response actions which could save lives and protect assets.

The ultimate aim of rapid identifiers is to achieve species level specificity, as this is required in order to distinguish disease-causing organisms (e.g., *Bacillus anthracis*, the causative agent of anthrax) from benign neighbors (e.g., *Bacillus subtilis*). Current methods that discriminate at the species level typically require incubation of lysed samples with reagents such as antibodies and nucleic acid probes. These sample manipulations are time-consuming (30-60 minutes) and thus preclude their use as rapid identifiers.

We have developed a novel identification methodology which does not require time-consuming lysing and labeling steps, but rather detects intact organisms using native near-infrared (NIR) absorbance and scattering. In this approach, organisms are sorted from each other and other particulates such as soot using capillary electrophoresis (CE), and detected by NIR absorption and scattering measurements.

There is substantial evidence in the literature that suggests that CE can be used to separate biological organisms by type and, albeit with fewer examples, by species (see for example, [1]). Successful separation by electrophoresis is dependent on the organisms having different net charge/mass. The challenge with species differentiation is that similar species are expected to be the same size, and thus separation depends on exploiting charge differences. Charge differences will arise from differences in protein, lipid and/or carbohydrate composition. For *Bacillus* spores, for example, there is surprising variation in the proteins comprising the spore coat. The number of spore coat proteins range from one major protein in *B. cereus* to more than 25 in *B. subtilis* [2]. Other differences include the presence in some but not all *Bacillus* spores of exosporium, surface layer, and filamentous structures [2]. *B. anthracis*, the causative agent of anthrax, is distinct from other bacilli in that the capsule is composed of poly-γ-D-glutamic acid rather than polysaccharide [3]. Although there is precedent for analyzing *Bacillus* spores by CE in the literature, the separation of different *Bacillus* spore species—and in particular, *B. anthracis*—is currently unreported.

The choice of NIR absorbance for detecting organisms is driven by the richness of the NIR spectrum for fingerprinting organisms and the availability and low cost of fiber-coupled NIR laser sources (diode lasers, fiber lasers, diode-pumped solid-state bulk lasers). UV absorbance is commonly used for detecting biological organisms; however, the UV region is not particularly spectrally rich for fingerprinting organisms despite being relatively strong. Additionally, UV light causes photodarkening of the fibers, greatly limiting their lifetimes. NIR spectroscopy, on the other hand, has been used extensively for identifying components in complex mixtures—e.g.,

glucose in blood, protein in wheat, and *E. coli* in fermentation broth. IR spectroscopy has been used to distinguish sporulated and vegetative states, and between different sporulated *Bacillus* species [4]. To pull out the often subtle spectral differences, multivariate pattern recognition techniques such as principal component analysis are required.

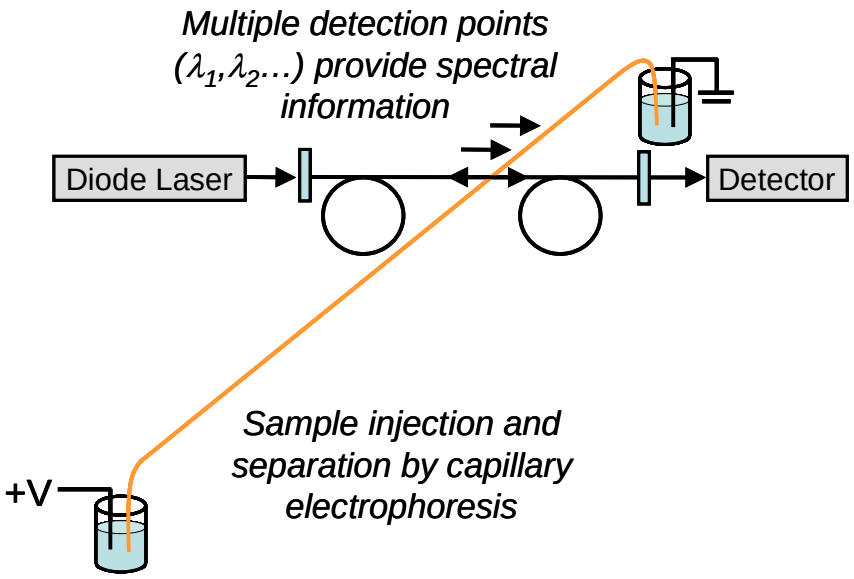

Figure 1 - The "MADNESS" rapid identifier system concept is based on CE separation of microorganisms and multi-wavelength NIR-CRDS detection.

In our approach, we propose to use multiple single wavelength fiber lasers to provide an effective "spectrum" from which to identify organisms (see system concept in Figure 1). For this LDRD we demonstrate the concept of near infrared cavity ring down spectroscopy (NIR-CRDS), near infrared incoherent broad band cavity enhanced absorption spectroscopy (NIR-IBB-CEAS) and near infrared single-pass detection of electrophoretically separated bacteria. One wavelength will be demonstrated, as this is sufficiently challenging for the level of funding. CE will provide the primary discriminating capability in this initial prototype device; however, we investigate NIR spectra of bacteria and viruses to identify a minimum set of wavelengths which will generate the requisite information for future devices.

A key challenge to implementing absorbance-based microfluidic approaches is achieving sufficient sensitivity, as CE absorbance pathlengths are short (<100 μm) and absorbance cross sections are relatively weak. To enhance the sensitivity, we will implement resonant cavity techniques (CRDS and CEAS). CRDS, a technique best known for gas-phase sensing, increases the effective pathlength for absorbance by one or more orders of magnitude by placing the absorber in an optical resonator; light injected from a laser into the resonator decays with a time constant related to the loss in the resonator, which includes absorbance from organisms. CEAS is a variant of CRDS, which directly measures an enhanced transmission loss, rather than an indirect loss via an exponential decay. Coupling of CRDS with fluid streams has only recently been reported. Studies which couple CRDS with HPLC have shown factors of 30-50 fold improvement over commercially-available absorbance detectors [5,6].

Detecting just a few bacteria will be challenging but not improbable with CRDS/CEAS (one bacterium detection has been claimed in the literature, for example). The challenge will be in reducing resonator losses as much as possible. Fibers provide a unique means of interfacing a resonant cavity to a nano liter detection volume of a micro fluidic flow. For fiber cavity ring down the optical resonator is formed as either a ring [7,8] or a "linear" cavity with mirrors [9] and fiber bragg gratings [10]; absorption by the analyte can be measured by breaking the fiber path and inserting the detection "cell".

In this report we describe the development of CE and resonant cavity methods for the sensitive and rapid detection of *B. anthracis* spores ("anthrax") in aqueous samples, and demonstrate an integrated prototype device.

EXPERIMENTAL

Materials and Reagents

Capillaries/cartridges, other consumables from Agilent, standard and square uncoated fused silica capillaries were from Polymicro buffers and other reagents were from Sigma and were analytical grade or better. Uncoated ~2 μm latex spheres and glass spheres (5200A and 9002) were obtained from Duke Scientific. Near IR dye (epolight 2717) was obtained from Epolin. Fluorescently labeled, carboxy-modified latex microparticles were obtained from Bangs Labs. Polyethylene oxide, MW 600K and 900K, were obtained from Fisher Scientific. Ready-made TBE buffer, containing 90 mM Tris, 90 mM borate pH 8.0 with 2 mM EDTA, was obtained from Invitrogen.

Biological Particles

Spores were acquired from Raven or Dugway Proving Grounds and used without further purification. They were stored in water at 4°C until use. Bacterial strains used for these experiments were primarily *Escherichia coli B* (ATCC 11303), *Bacillus subtilis* 168 (ATCC 23857), *Bacillus cereus* (Raven Labs), and *Bacillus globigii* (obtained from Dugway Proving Ground). Vegetative samples of each strain were grown in Luria Broth to mid-log phase (A600 = 0.4-0.7) at 37ºC with shaking. Cells were harvested by gentle centrifugation to avoid cell lysis (5 min at 1000 g) and washed by resuspending once in TBE buffer and once in distilled water to minimize contributions from growth media. More extensive washes were avoided to minimize impact on the cells. Final concentration of the sample buffer was ~ 0.1 x TBE buffer.

CE separations

CE separations were performed on an Agilent 1600 series Capillary Electrophoresis System with a UV/Vis absorbance photodiode array detector. A range of wavelengths were simultaneously monitored during electrophoresis; they typically included 200 nm, 214 nm, 254 nm, 280 nm and 488 nm. Electrophoresis was carried out using a 100 μm ID capillary, 33 cm in length total with a 26 cm distance between the inlet and the detection point loaded into the standard Agilent capillary cartridge. Separations were run at 15 kV in normal mode (electroosmotic flow or EOF toward detector). Before each run, the capillary was flushed with 1 N NaOH (1 min at 20 psi) followed by running buffer (3 min at 20 psi). Injections of suspensions of cells and spores were by pressure, typically 33 mbar for 3 seconds. The running buffer was TBE to which a series of concentrations of PEO (0 to 0.1% (w/v) and either 600k MW or 900 k MW polymer) was added.

A dilute solution of mesityl oxide was used as an EOF marker and injected at the end of the pre-run flush steps.

IBB-CEAS setup

Near IR radiation was generated with a 1054 nm superluminescent light emitting diode (SLED) (QPhotonics 2 mW, 35nm FWHM). An SLED is a guided-wave semiconductor device similar to a laser diode that lacks the optical feedback required for lasing. The SLED structure provides beam divergence and output power comparable to a single-transverse-mode laser diode, but low temporal coherence and broad spectral emission of an LED.

The SLED was operated with a constant current of 60 mA and temperature of 25°C (ILX Lightwave LDC-3724B controller). The output of the SLED was sent through a fiber-coupled polarization independent isolator (OFR IO-F-1064) to prevent back reflections from destabilizing the SLED output. Without the isolator, the back reflection caused additional background noise. The output of the isolator was launched into the IBB-CEAS cavity using a +8 mm aspheric lens to collimate and a +11 mm corresponding lens to re-image onto the cavity face. Alignment into the cavity was highly sensitive to position, particularly in the plane (X-Y) transverse to the fiber axis (Z). X-Y-Z alignment was facilitated by a flexure mount with micron adjustment resolution. Angular alignment was performed using a pitch-yaw stage attached to the flexure mount.

The optical cavity was formed by butting mirrors (1/8" thick, 98.9% reflective at 1054 nm) to the ends of optical fibers using Luvantix PC-452 optical polymer for index matching. The optical fiber had a graded index (GRIN) profile with core and cladding diameters of 62.5 and 125 μm respectively (OFS Optics). The total fiber length was 11 cm, which was cleaved in half with a diamond cleaver and separated at the cleave by 70 μm to form the sample region. Alignment of the mirrors to the fiber was done using translation stages and the aid of a video microscope.

The axes of the two fiber halves were aligned using a vacuum chuck with a v-shaped groove. The vacuum held the fiber firmly in the channel as the cleaved ends were separated by the desired amount. The fibers were then immobilized with UV-cured epoxy to within approximately 1 mm of the gap. The fiber gap sat in a well of approximately 50 μL volume to hold the samples. The sensing volume between the fibers within the well was approximately 0.2 nL. Sample solutions were introduced into the sample well within 20 μm of the fiber gap via a 100 μm ID fused silica capillary. Solutions were injected into the capillary using a syringe.

The output of the cavity was re-imaged with +11 mm aspheric lenses through a 980 nm LPF onto an unbiased Si photodiode. The signal was then amplified (Melles Griot Large-Dynamic Range Photodiode Amplifier) and sampled using a National Instruments DAQ (USB 6009 or PCI 6014). Labview was used to acquire the data stream, and data were post-processed in Wavemetrics IGOR.

CRDS setup

The CRDS setup was similar to the IBB-CEAS setup with the following four component substitutions: (1) NIR radiation was generated at 1550 nm with a New Focus Velocity tunable laser diode which was modulated on and off with an acoustic optical modulator (AOM); (2) the cavity used 1/8" thick, 99.0% mirrors reflective at centered at 1550 nm; (3) the optical fiber

length was varied between 100 and 3 meters to tune ring down times; and (4) the signal was measured using a Thorlabs PDA10CS InGaAs current amplified photodiode

Graded index fiber gap launching characterization

Graded index fiber has been shown to propagate radiation across a gap with high efficiency while maintaining low order mode character [11] and being able to maintain its mode structure over long distances of fiber with minimal mode mixing [12]. To demonstrate this with our GRIN fiber, a single mode source was launched through a section of graded index fiber with a water filled gap, and both the transmission loss and the beam profile were measure with a photodiode and Data Ray WinCam imager for various gap distances. To prevent cladding propagated light from artificially enhancing the transmission loss, mode stripping was done both before the gap and again after the gap, and before the detector.

Limit of detection and IBB-CEAS enhancement factor

The IBB-CEAS measurement was characterized as a function of sample absorption using a water-soluble near-infrared dye, Epolight 2717. This dye allowed us to control the absorption in an aqueous sample without substantially changing the index of refraction, and thus isolate the effect of sample absorption and ignore refractive changes. For a given concentration of dye, an alternating flow of dye and water was sent into the fiber gap both to establish the background and to measure repeatable absorptions. This was done both for a mirrored cavity and a mirror-less cavity. The ratio in transmission was used to determine the cavity enhancement factor for the system. As discussed below, the limit of detection (LOD) was inferred from the background noise level.

To investigate the IBB-CEAS's performance with particulate mater, polystyrene and glass spheres were used with diameters of approximately 2 μm, comparable to many biological organisms of interest. The spheres were first diluted to about 1 μg/mL and then flowed over the gap the fiber gap. By using a sufficiently dilute suspension of particles, we were able to resolve individual particles passing through the gap.

RESULTS

Capillary electrophoresis

CE separation of Bacillus spores and vegetative cells

A survey of the literature has shown that presence of small amounts of polymers (e.g. polyethylene oxide or PEO) in the running buffer has the effect of dramatically enhancing the resolution of intact vegetative cells, sharpening the peaks in by one of several possible focusing type mechanisms [1]. Given the very high resolution, it may be possible to "identify" organisms directly from characteristic electrophoretic migration times. We have sought to extend this capability to bacterial spores as well as vegetative cells since there is a strong interest in being able to detect spores; the spore former *B. anthracis* represents one of the highest bioterrorism concerns.

We evaluated a range of PEO concentrations from 0 to 0.1% (w/v). Figure 2 shows the effect of increasing PEO concentration on the migration. Higher PEO concentrations tended to speed up

the migration times of spores, apparently coating the spores and making them more neutral overall. In addition, higher concentrations of PEO appeared to have the effect of reducing the number of peaks present in the separations. Interestingly, in the case of spores, peak width did not significantly decrease with increasing PEO concentration in contrast to what has been reported for vegetative cells. This may indicative of the morphology of spores to begin with, being more particle-like than the vegetative cells; spore peaks were very sharp even in the absence of PEO.

We also evaluated the impact of the polymer molecular weight on the resolving power. We used solutions made from both 600,000 and 900,000 molecular weight. The overall the performance seemed comparable, although the viscosity of a 900 kD polymer at the same concentration was noticeably higher. We settled on using a 0.1% PEO solution made using 600 K MW polymers. This was chosen as the largest concentration of PEO that did not appreciably impact the viscosity of the running buffer. High viscosity in the running buffer was seen as undesirable because 1) it would unnecessarily slow the separations and 2) complicate the separations due to the possible contributions of sieving expected with high viscosity polymer solutions.

It was necessary to determine the level of discrimination possible and this was evaluated first with spores because of their relative ease of handling. Figure 3 shows the traces for three different spores, each showing a different migration time for the major peak in the electrophoretic trace. The migration times of the major peak in the *B. cereus* sample and the *B. anthracis* sample are much closer to each other than they are to *B. globigii*. This is seen as encouraging since the former two organisms are much more closely related to each other than to B. globigii. We also saw comparable, apparent species level discrimination of other organisms including three species of diatoms shown in Figure 4. Three separate traces are shown for the individual diatom samples. A trace containing three peaks was generated for a mixed sample.

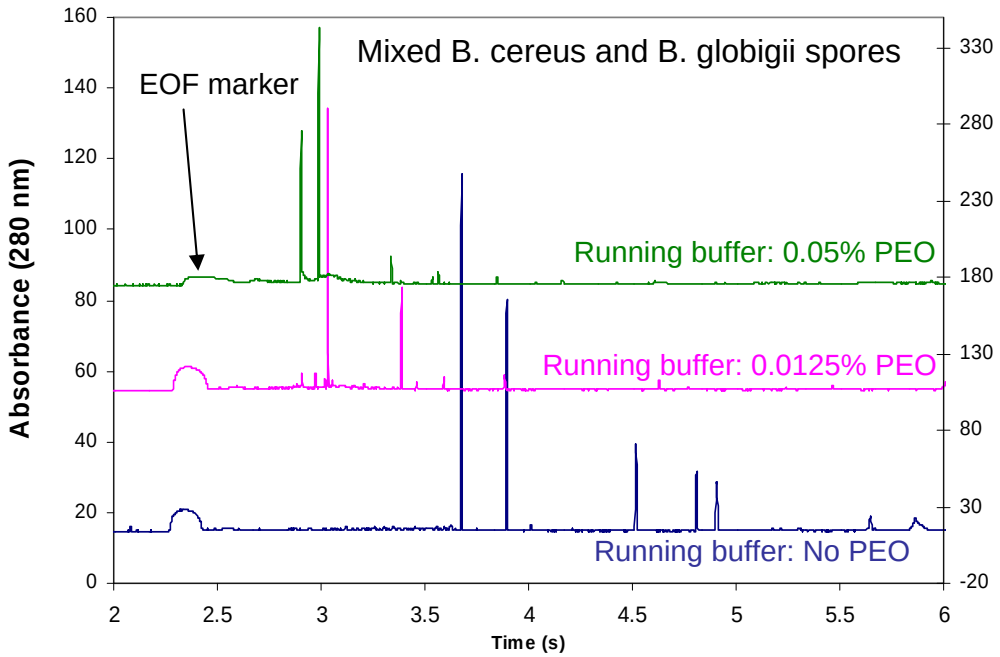

Figure 2 - The effect of polyethylene oxide (PEO) on the electrophoretic migration of B. cereus and B. globigii spores.

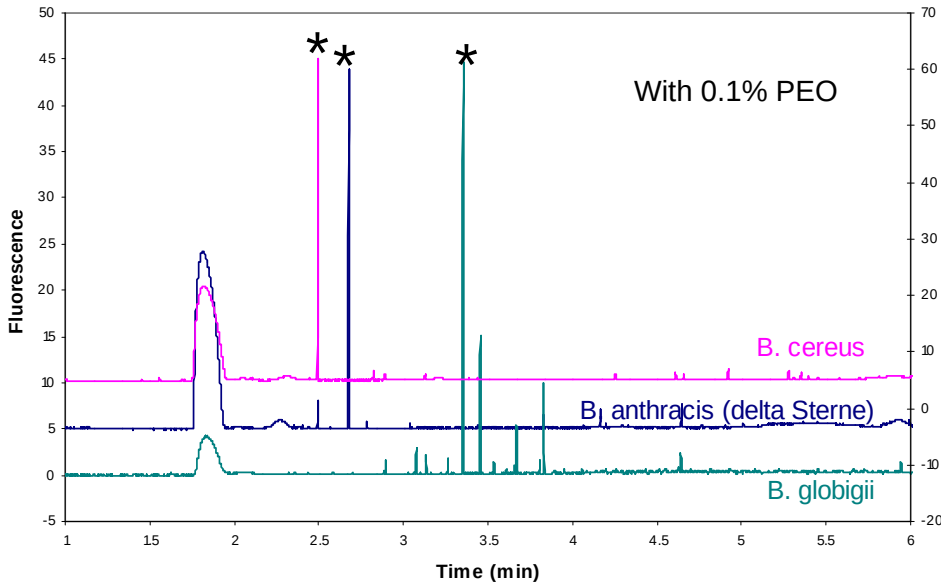

Figure 3 - CE separation of different Bacillus spores: B. cereus, B. anthracis (delta Sterne) and B. globigii.

Figure 3 also illustrates the persistence of smaller later-eluting peaks that were highly variable in migration time and intensity. It was initially assumed that the additional peaks represented aggregates of spores but microscope analysis of suspensions of spores revealed typically single spores and only very small clumps of spores, typically two and three in number. Sonication appeared to help this, especially when the sample matrix was water; however, we have not been able to eliminate the presence of additional peaks completely.

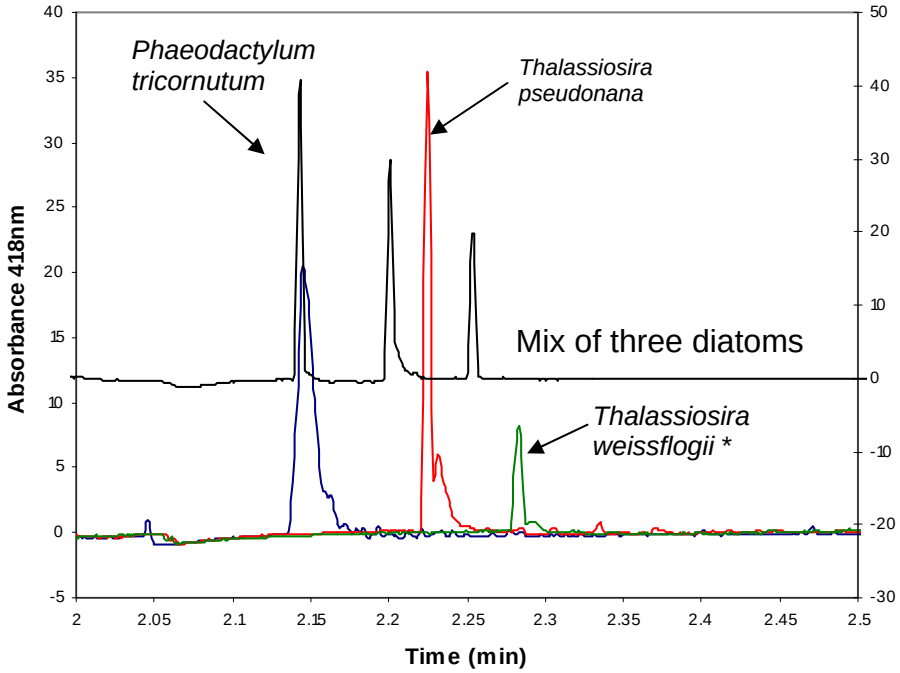

Figure 4 - CE separation of different diatoms using the same method as for Bacillus spores.

Method robustness for Bacillus spore detection

Regardless of the presence of additional spurious peaks, if the reproducibility of the primary peaks is sufficient then it should still be possible to use migration time to identify spores based on migration time, provided appropriate "windowing" is used. We sought to evaluate the overall reproducibility of migration times for a suite of spores, including *B. cereus* and *B. globigii*. Given the sharpness of the peaks, it was desirable to have migration markers to correct for minor run-to-run variations in electrophoresis which can result from environmental factors such as ambient room temperature and sample matrix.

The first marker used was mesityl oxide, a neutral molecule commonly used as an electroosmotic flow (EOF) marker. Reproducibility was not high with just one internal standard; consequently we sought to include a second internal standard, preferably one that migrated after the last biological particle of interest. A variety of particles were evaluated for this purpose including fused silica beads and polystyrene latex beads, both of which were not detected either because of being essentially transparent (fused silica) or uncharged (polystyrene). We acquired mono-disperse polystyrene latex beads (50 nm and 300 nm) that were surface carboxy-coated (negative charge) and modified with a fluorophore to aid identification. While these spores migrated sufficiently late to be a good internal standard, their electrophoretic migration resulted in multiple broad peaks and reproducibility, especially in presence of biological samples was poor. Negatively-charged small molecules were next evaluated and fluorescein was found to be much more successful as a second standard. It retained enough absorptivity at 280 nm to be detected on the same channel as the particles and the EOF marker (Figure 5).

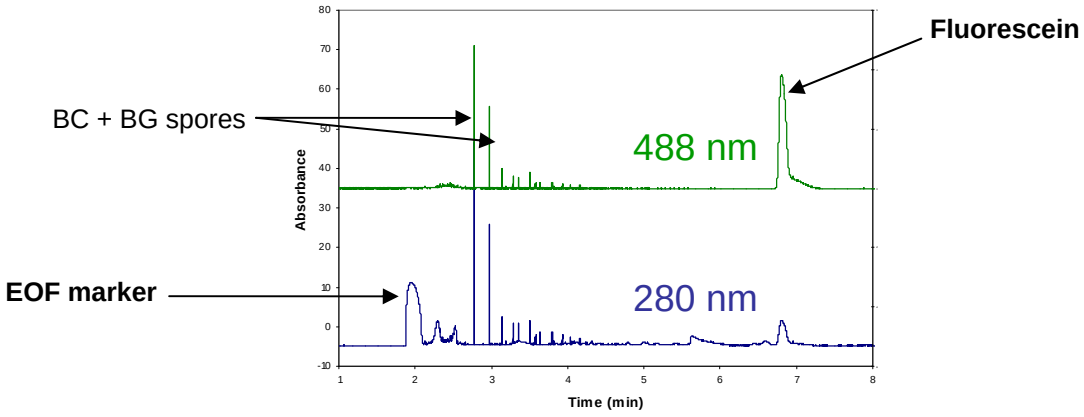

Figure 5 - Internal standards used for the reproducibility study were mesityl oxide, an EOF marker, and fluorescein dye.

A relatively large reproducibility study was carried out using both the EOF marker and *B. cereus* and *B. globigii*. The results, shown in Table 1, indicate individual spore peaks are detected and more reproducible even when two spores were mixed in the same sample. While this is encouraging, spores still demonstrated higher than ideal level of variation, with a standard deviation of approximately 0.2 minutes. Compared to the overall migration time (~6%) and sharpness of the peaks, this seems quite high. It is possible that some of this variation is due to the particulate nature of spores. Spore surface effects (surface charge) may not be fully

controlled under CE conditions (e.g., the extent of PEO coating of the spores) and the spores' behavior may be complicated by non-electrophoresis effects or particle dynamics. For example, particle effects such as settling have been seen to affect CE results; e.g., a freshly suspended sample will yield a somewhat different pattern of peaks than one that has remained untouched for 15 minutes or more. How much this can be expected to impact variability during the capillary separation is unclear, but it will almost certainly impact the observed reproducibility. Regardless, it may be possible to "window" the detection, given that, at least for the two species show in Table 1, the average migration times are approximately two standard deviations away from each other.

Table 1 – Reproducibility of B. cereus and B. globigii spore peaks alone and in combination using 2-pt correction.

Spore Type	***Major Peak(s) (Std Dev)***
B. cereus	3.02 (0.19)
B. globigii	3.41 (0.25)
B. cereus + B. globigii	2.99 (0.20), 3.41 (0.23)

We also sought to explore the level of discrimination possible with mixtures of spores and vegetative bacteria. Several different types of vegetative cells were cultured and harvested at mid log growth and mixed with different spores. Similar to the purely spore samples, we anticipated being able to see peaks that we could associate with the individual component cell types in the mixtures; unfortunately the situation was much more complex. Mixtures of *B. globigii* and *B. cereus* spores with assorted vegetative cells showed significantly greater variability, and it was difficult to identify peaks associated with the spores from the mixed samples, even with two-point migration time correction. A number of issues may be at play: not fully controlled particle behavior as described previously; vegetative cells with different settling dynamics than spores; protein mediated interactions between spores and cells; interaction of residual growth media with cells and spores that impacts the PEO coating process; and possible germination of the spores in the presence of other organic matter [13,14]. The issue of possible germination is something that is specific to spore containing samples; it can not be ruled out at this point, but can be determined in the future with relatively simple experiments using a phase contrast microscope to image the cell and spore mixtures over time and CE time-course experiments.

Certainly understanding the behavior of cells in mixtures has implications for biodetection in general. Follow on experiments will need to address these issues of reproducibility and answer the question about whether cells are interacting in the sample matrix. It will be necessary to decouple and better control particle dynamics of cells. Also it will be necessary to determine if there are conditions which will allow better reproducibility and that can be applied to sample preparation of unknown mixtures of cells.

Cavity enhanced absorbance method development

NIR wavelength selection

Analysis of NIR spectral features of bacteria [15-17] suggests three candidate wavelengths for detection: ~1064, 1550 and ~1660 nm (Figure 6). Because of the strong water absorption at 1550 nm and above, better sensitivity is expected at 1064 nm. These wavelengths will be evaluated for their ability to discriminate organisms using CRDS.

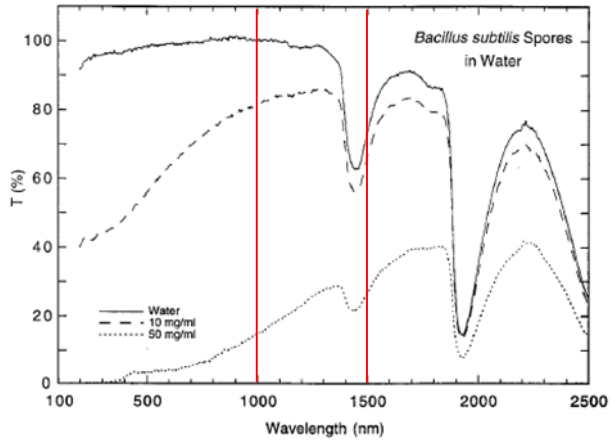

Figure 6 - Optical spectra for Bacillus subtilis spores in water. Taken from [15].

Overview of fiber devices development

Initial experiments on developing fiber-CRDS was on minimizing the loss of the cavity to maximize sensitivity. It was found that lensing the fiber ends provided little benefit for fiber-to-fiber transmission. By monitoring the transmitted power for various gap distances and mode patterns, it was determined that a graded-inded multimode fiber had good transmission with simple cleaved ends.

Fiber-CRDS was first performed using a 10 m fiber cavity using 1.5 µm light (schematic of the set-up is shown in Figure 7). The ringdown times were stable at ~10 µs. This system had good sensitivity in the 1.5 µm water-loss dominated NIR region, which may be valuable for water content diagnostics. Fiber-CRDS at 1.0 µm was also investigated, as this wavelength would have a stronger NIR protein absorption and minimal water absorption; however, it was found to have unstable ring down times. As an alternative to CRDS, IBB-CEAS was investigated. This technique variation allowed for very short fiber cavities (several centimeters vs several meters) and resulted in stable transmission at 1.0 µm.

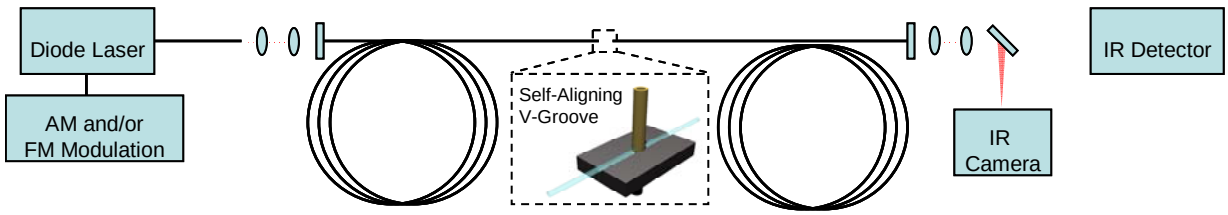

Figure 7 – Schematic of the fiber-coupled CRDS set-up.

Graded index fiber gap launching characterization

The effect of light propagation across the gap in the fiber was studied using segments of GRIN fiber with no mirrors. Figure 8 is a plot of transmission loss through two segments of GRIN fiber separated by water as a function of gap distance corrected for the loss of the water. Loss due to water was subtracted from the measured loss in order to separate out the loss due to beam divergence across the gap. Figure 9 is a series of images of the fiber output mode pattern for gap separations in the range of 0 μm to 200 μm for the single-pass setup. It can be seen in Figure 8 and Figure 9 that for a single pass and a gap separation up to 200 μm, the graded index fiber propagates with almost no transmission loss and maintains a Gaussian-like superposition of modes having a strong central weighting.

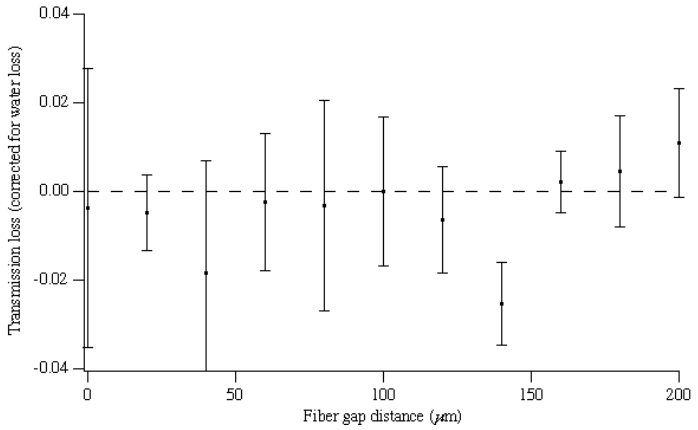

Figure 8 - Transmission loss across a variable distance water-filled fiber gap after correcting for water absorption loss.

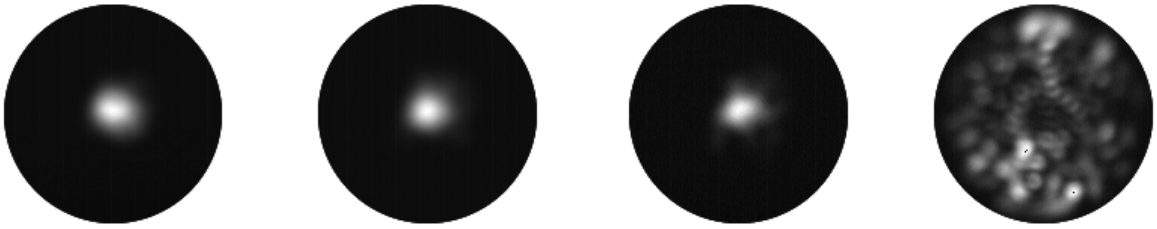

Figure 9 - Exit beam profiles of single mode light launched into a multi-mode graded index fiber containing a sample gap. Gap distances from left to right are 0, 100, 200 um spacing and an intentional translationally misaligned gap to show high order modes.

The selective excitation of low order modes by single mode launching into graded index fibers is known for its importance with applications in the telecommunications industry [18-21]. It has been shown that the expanded mode from a gapped launch from a single mode fiber to a graded index fiber launches into higher order modes, indicated by its bandwidth reduction [22].

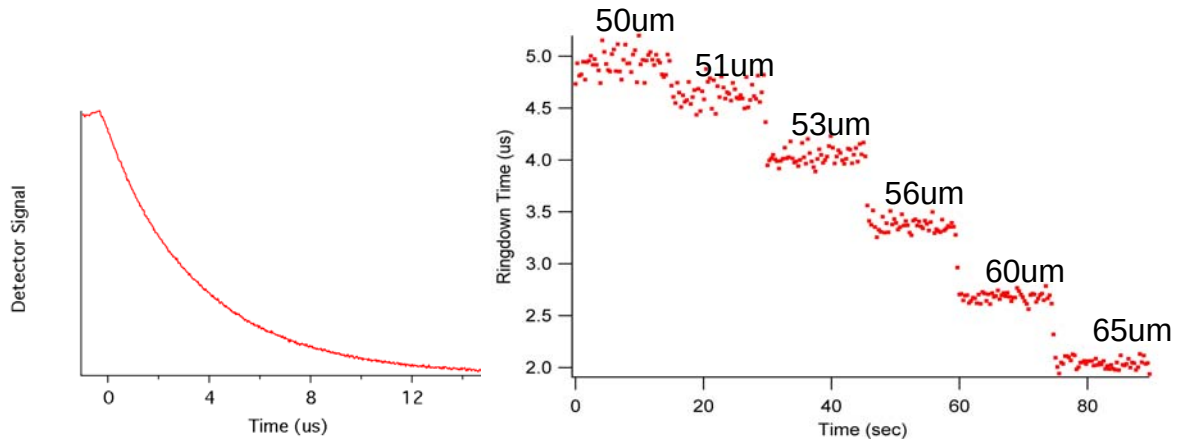

Figure 10 - (A) Representative ringdown signal. (B) Water transmission for different pathlengths.

CRDS vs. IBB-CEAS

CRDS uses a modulated optical input signal and indirectly measures absorption using either the decay rate or the phase shift of the transmitted signal. While this technique is independent of any power fluctuations, it is susceptible to modal and temperature noise associated with the long fiber lengths used to stretch the ringdown time or phase shifts to practical values. This method also requires relatively fast data acquisition electronics and a modulated laser source. CEAS, a variant of CRDS, measures the average transmission through the cavity. The CEAS transmission signal is directly proportional to input power, making the technique sensitive to input fluctuations, but a correction can be applied using a simultaneous measurement of the input power.

Incoherent Broad-Band CEAS (IBB-CEAS) has been demonstrated previously for gas [23-26] and bulk liquid [27] samples; however, these implementations were not designed to address the challenges associated with small, dynamic detection volumes inherent with separation techniques such as capillary electrophorisis or high-pressure liquid chromatography. In this work, we describe a fiber coupled IBB-CEAS optical detector for microseparation analysis such as capillary electrophoresis.

Integrated CEAS

An integrated cavity is preferred to a discrete component cavity due to its smaller size and increased robustness for a fieldable device. The original CEAS setup used discrete optics to form the fiber cavity, and translation stages and lenses to launch light into the fiber, and out to a detector. This setup allowed for systematic experiments to characterize the properties of the cavity and determine design parameters for an integrated cavity.

The integrated optical cavity was formed by directly depositing mirrors onto a cleaved 10 cm segment of GRIN fiber, having a reflectivity profile maximized for sensitivity. The optical and translational components used for re-imaging the launch laser onto the cavity were replaced by a single-mode, large-mode-area fiber having a mode field diameter comparable to the lowest order mode of the GRIN fiber. This allowed butt-coupling of the launch fiber directly to the mirrored cavity, using index-matching polymer. The output components were similarly replaced with a

butt-coupled multimode fiber, which was connected to an integrated current amplified photodiode.

Performance of the integrated CE-CEAS prototype

Flow cell development

Similar to the development of the fiber-based cavity enhanced detection techniques, integration of the fiber cavity to a microfluidic flow had an evolutionary pathway. The initial proposal was to use a micro-cross cell to interface the optical and fluidic channels; however, it was found that the fiber-to-fiber alignment was very sensitive to micron level misalignments which were inherent in the micro-cross scheme. The development of passive fiber-self-aligning precision-machined fiber v-grooves solved the alignment problem but required a new method to integrate the fiber to a capillary.

Initial work on integrating the fiber and capillary involved laser micromachining counter bores into the sides of a capillary; however, the drilling process resulted in large surface imperfections that were incompatible with a resonant cavity. An alternative interface was then developed which used a drilled capillary sleeve to mate the fibers, capillary, and v-groove (Figures 11 and 12).

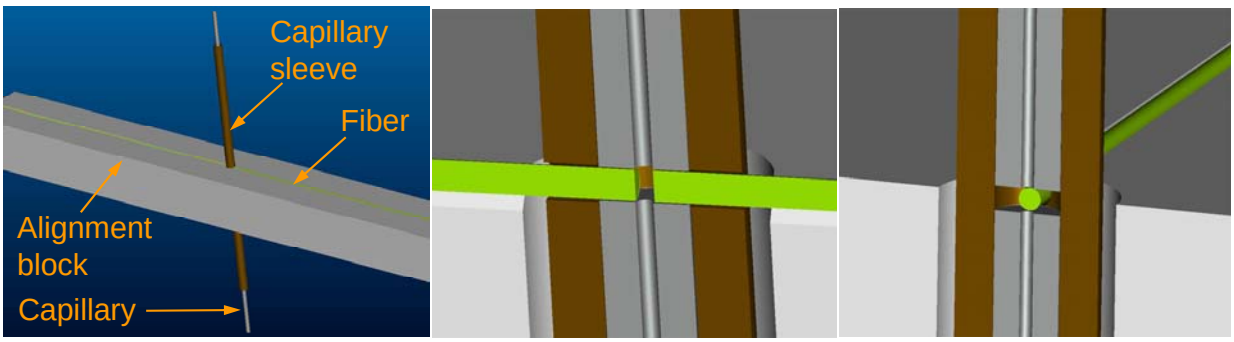

Figure 11 – CAD drawing of the integrated capillary-fiber CEAS prototype shows the capillary-fiber junction. A small gap is created in the capillary at the fiber junction, which is not ideal, as it may allow particles to collect and be difficult to remove.

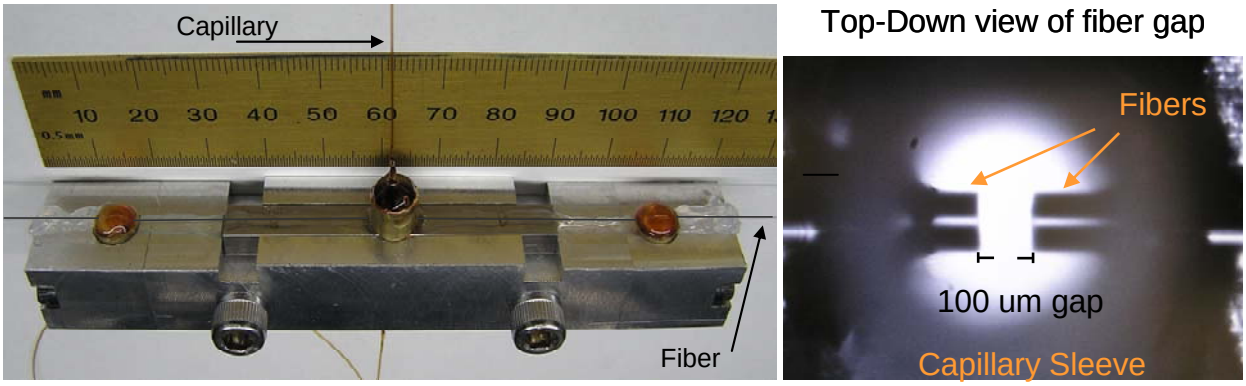

Figure 12 – Pictures of the actual integrated capillary-fiber CEAS device.

NIR dye characterization

Epolight 2712 was diluted in distilled water to concentrations ranging from 1.2 mg/mL to 420 ng/mL for IBB-CEAS sensitivity measurements. These solutions were measured in a 1 cm cell with the 1054 nm SLED as the radiation source (Figure 13) and the absorption coefficient was determined to be $\varepsilon = 8.4$ L g^{-1} cm^{-1} with respect to base-e as (or approximately 6.7 $x10^3$ L mol^{-1} cm^{-1}. The exact molecular mass is proprietary information, but it has a value of 800 amu +/- 5% [28]) which is consistent with published values.

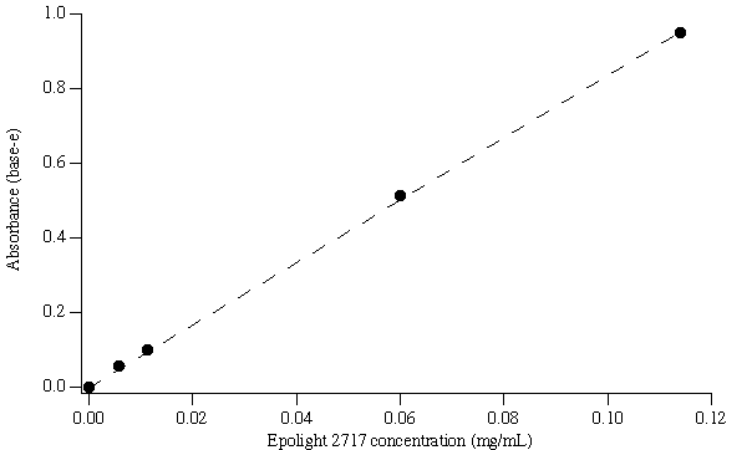

Figure 13 - Calibration curve for Epolight 2717 through a 1 cm cuvette using the 1054nm SLED for the radiation source

The ability of the technique to detect low absorbances (Figure 14) was demonstrated by measuring the transmission of an alternating flow of distilled water and dye solution. The completeness of the dye removal during the distilled water flush is indicated by the return of the background to its original level (Figure 15a). The discontinuity in the flow caused by changing between sample and distilled water imparted an additional variation in the signal that would not be present during a measurement using a continuous flow such as electrophoresis. Therefore, we inferred the LOD from the background noise level (Figure 15b).

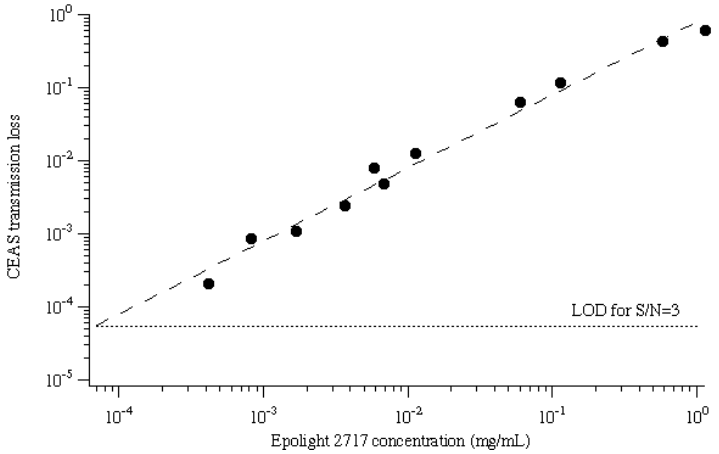

Figure 14 - Transmission loss measurements over ~4 orders of magnitude of dye concentrations. The dotted line represents the LOD for a signal-to-noise ratio of 3.

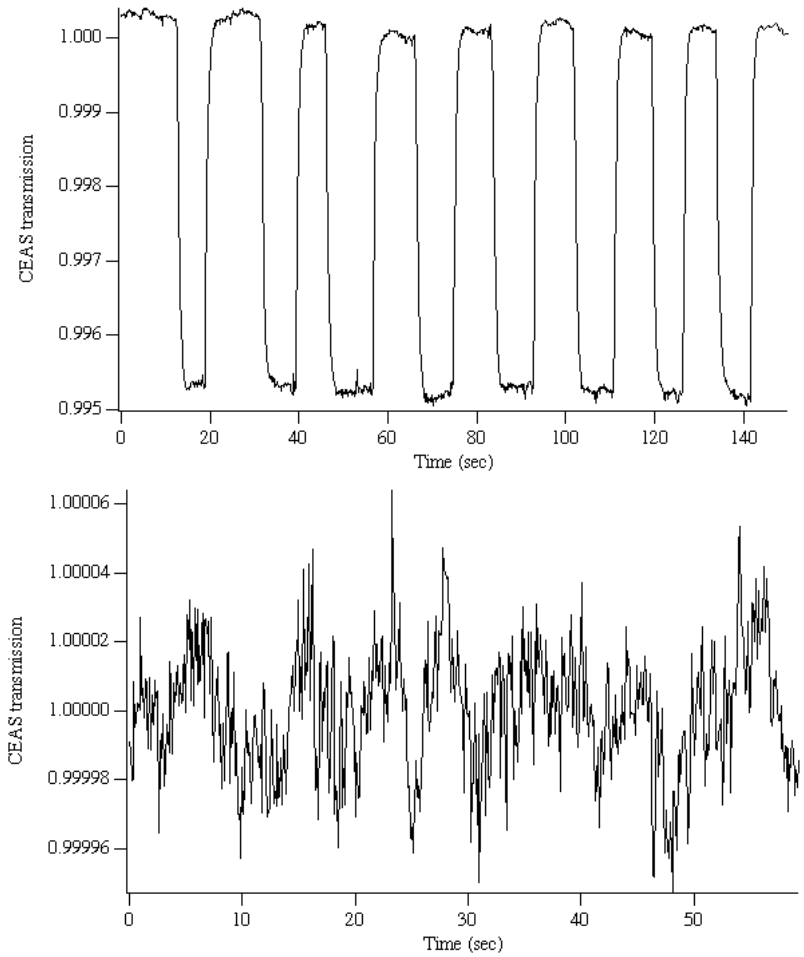

Figure 15 - (A) Measurement of successive alternations of water and 6.8 µg/mL solution of Epolight 2717 dye through the detection gap. (B) Drift corrected background signal of static water in the detection gap, used for LOD calculation.

A continuous data set was acquired for 60 seconds at 0.1 second integration time per point. The data were normalized to the slowly drifting background using a 2nd order polynomial correction. The standard deviation of the noise was taken, and for a signal-to-noise ratio of 3, the LOD of the smallest measurable IBB-CEAS loss was 5.5×10^{-5}, which corresponds to approximately 70 ng/mL. For the sample path length of 70 µm and extinction coefficient of 8.4 L g^{-1} cm^{-1}, this is equivalent to a single pass absorption of 4.1×10^{-6}.

The enhancement factor was measured as the ratio of the losses of a resonant cavity to that of the cavity with the mirrors removed. Since the fiber-mirror interface was indexed matched, and there was no AR coating on the non-contact face of the mirror, there was no need to make corrections for back reflections for the new air-glass interface. The enhancement factors for concentrations between 1.2 and 0.006 mg/mL (where single pass measurements could be made) are shown in Figure 16. For small transmission losses, this device has an enhancement factor of approximately 9.

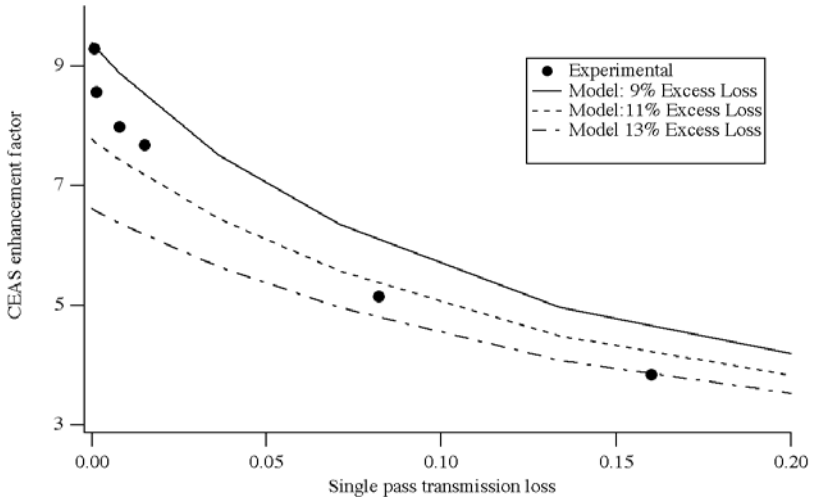

Figure 16 - Experimental enhancement factors for the CEAS detector as a function of transmission loss compared to model enhancements for a range of excess losses.

The enhancement factor was modeled for the IBB-CEAS system using a linear-loss resonator transmission model. The calculation was done across the bandpass of the SLED as an integral of normalized enhancements accounting for the wavelength dependence on mirror reflectivity, dye extinction coefficient, and SLED intensity. Experimental enhancement factors were compared to model predictions, and the results were found to be in poor agreement. A more complex model needed to account for additional loss mechanisms.

The detection limit of the described IBB-CEAS system compares very favorably to related works using optical fibers in an enhanced scheme to detect dilute aqueous solutions (Table 2). Compared to other works, the minimum detectable absorption loss (MDAL) of this work is lower by two orders of magnitude. We believe the lower LOD reported here is largely due to a combination of lower system losses and higher optical stability of the approach.

Table 2 - A comparison of various resonance-enhanced, fiber coupled systems used to measure aqueous solutions in the near-IR. Values reported are for attained LODs and not theoretical instrumental limits. The LOD for the integrated IBB-CEAS was electronic noise limited.

Technique	***Compound***	***λ*** ***(nm)***	***Ext Coef (base-e)*** ***L/(mol*cm)***	***L*** ***(μm)***	***LOD*** ***(μM)***	***MDAL*** ***(cm^{-1})***	***LOD Equiv Absorbance***
Pulsed CRDS [4]	Methylene Blue	660	$1.5x10^5$	100	50	7.5	$7.5x10^{-2}$
Fiber Loop CRDS [2]	DDCI	825	$3.3x10^5$	3.8	270	90	$3.3x10^{-2}$
Fiber Loop CRDS [18]	DDCI	825	$3.3x10^5$	35	6	2.0	$7.0x10^{-3}$
Phase Shift CRDS [19]	ADS805WS	810	$1.9x10^5$	10	5	0.8	$9.5x10^{-4}$
(Discrete) IBB-CEAS	Epolight 2717	1054	$6.7x10^3$	70	0.088	0.0006	$4.1x10^{-6}$
(Integrated) IBB-CEAS	Epolight 2717	1054	$6.7x10^3$	100	0.22	0.0015	$1.5x10^{-5}$

Particle detection

As a proxy for cells, spores and other bioparticles, polystyrene and glass spheres were introduced to the water-filled sample well just above the fiber gap and were allowed to settle passively through the detection region. The glass spheres were 2±0.1 µm, and the polystyrene spheres were 2±0.7 µm. Figures 17a and 17b show the high sensitivity to particle detection. The width of transmitting dips is likely due to the rate at which the particles moved through the fiber gap. The surfactant coated polystyrene spheres with a density 1.05 g/cm^3 would pass through the gap via "slow" Brownian motion. The glass spheres, on the other hand, have a density of ~2.6 g/cm^3 and could settle through the gap in a more direct path at a faster rate. Since neither material has an appreciable absorption over a 2 µm path length, scattering dominates over absorption loss.

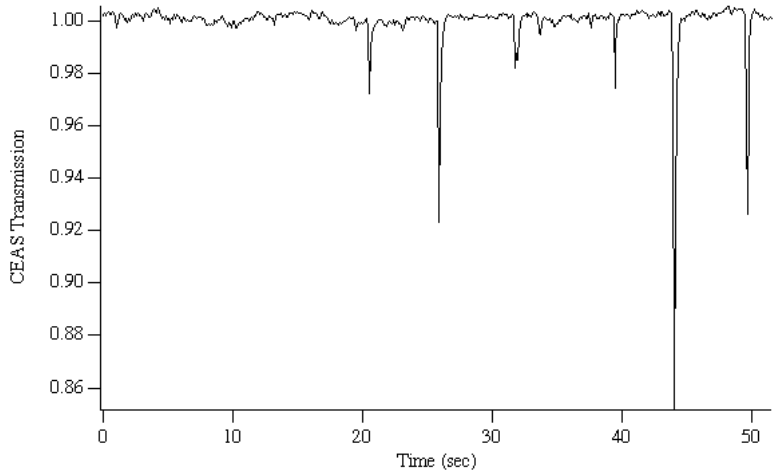

(A)

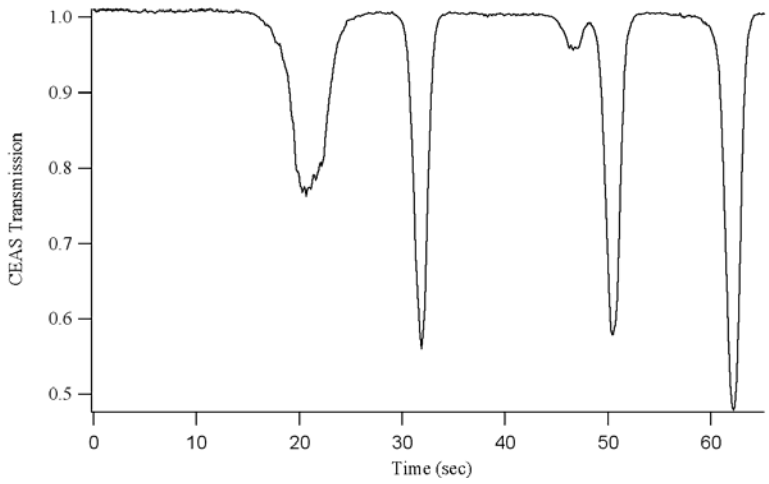

(B)

Figure 17 - CEAS measurements of 2 µm polystyrene (A) and glass (B) spheres.

Single pass measurements on CE separated spores

Although preliminary work done on CE through the integrated fiber-capillary junction indicated that the interfacial discontinuities did not affect the spore peak widths or times in any substantial

way, more extensive CE measurements revealed complications with clogging and inconsistency likely due to the fiber protrusions into the electrophoretic flow. Reasons for the later problems include subtle differences in the CEAS set-ups between the two sets of analyses, and problems associated with letting the set-up sit for a periods of time.

Exploratory experiments indicated that the transmission loss for a sample containing spores was dominated by scattering. Spores are comparable in size to the wavelength being used and have an index of refraction contrast to water, giving them the potential to scatter light elastically. Spore scattering could be detected without an enhanced setup. The ability to distinguish between different organisms would likely require the ability to measure changes in transmission at different wavelengths with high precision and sensitivity. Because we were unable to use the fiber CEAS setup with CE without clogging the capillary, we decided to investigate the signatures of organisms on a single pass with a continuous capillary.

We developed a simple configuration that allowed CE to be performed on organisms and measurements to be made of their extinction and large-angle scattering. Light was launched out of a low NA, single-mode fiber through a polyminide stripped square capillary and into a receiving multimode fiber (Figure 18). However, unlike the IBB-CEAS setup, this single pass configuration disrupted neither the CE field nor flow.

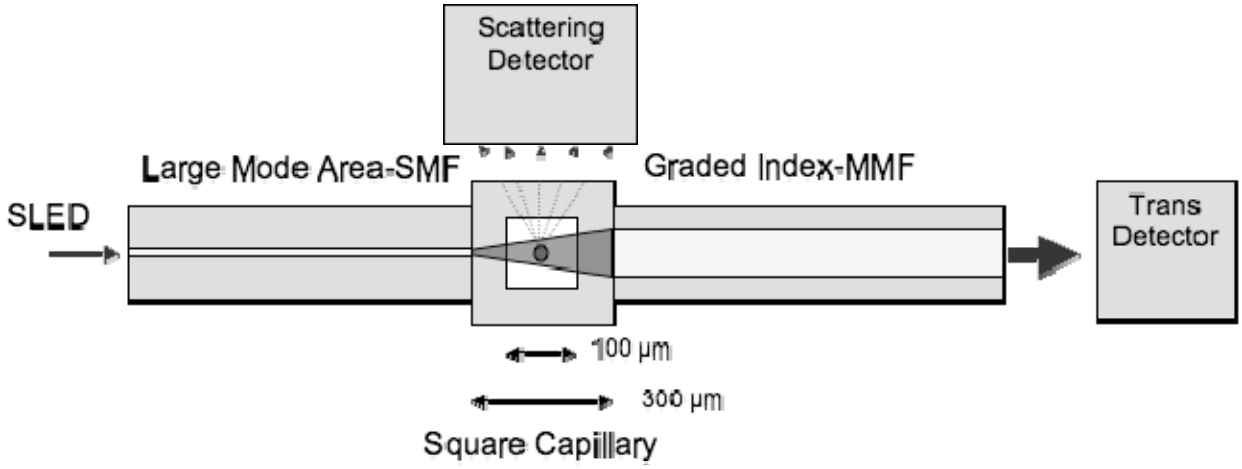

Figure 18 – Single pass setup used to simultaneously measure transmission loss and scattering of light by CE separated spores

The single pass arrangement allowed for simultaneous scattering and transmission loss measurements (Figure 19a). When expanded to multiple wavelengths, the scattering and transmission ratios (Figure 19b) might be able to be used as an identification parameter. Scattering measurements were performed on a size series of latex spheres. These measurements indicated that for sphere-like particles with an index of refraction similar to latex, the LOD is between 300 and 500 nm.

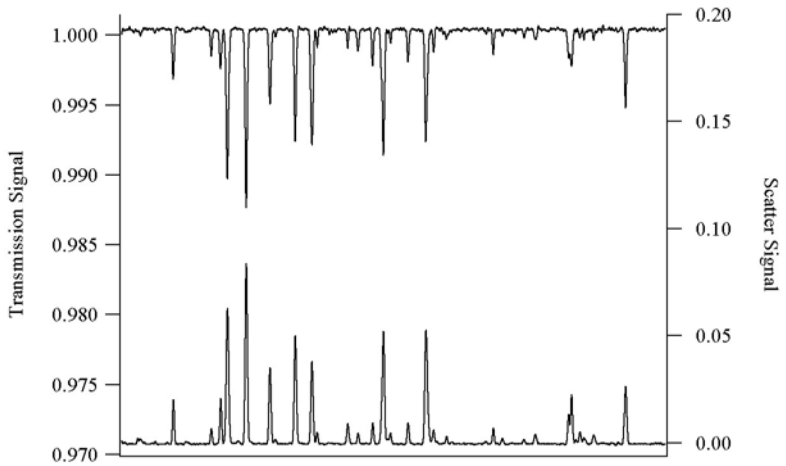

(A)

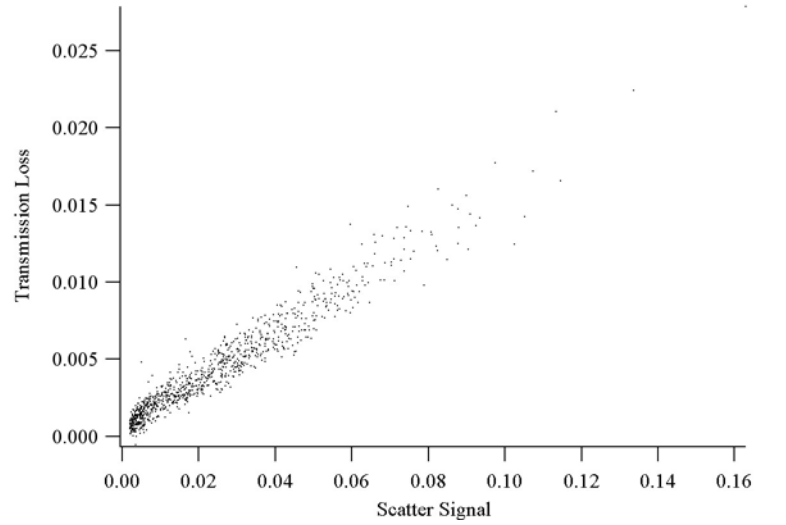

(B)

Figure 19 – (A) Single pass transmission and scattering measurements for 1.8 µm latex spheres. (B) Characteristic transmission-scatter relationship for B.Cereus at 1.0 µm

Scattering/transmission measurements were also performed on CE separated *B. cereus* spores. Because of the time resolution of the system, both spore counting and width measurements were possible (Figure 20). This width parameter adds an additional level of discrimination and may be used to ascertain size information of a particle.

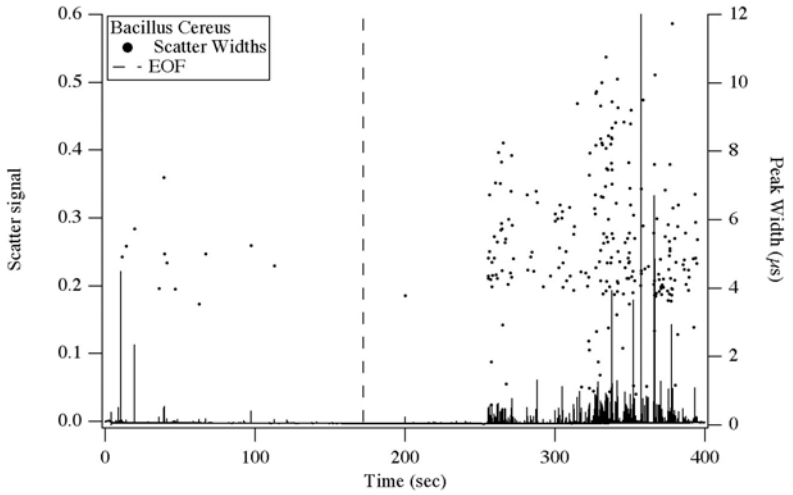

Figure 20 – Single pass scattering and peak width measurements for CE separated B. Cereus.

CONCLUSIONS

We have developed a rapid (1-5 minute), novel identification methodology that sorts intact organisms from each other and particulates using capillary electrophoresis and detects using NIR absorbance and scattering. To prove this new methodology, we have successfully demonstrated CE resolution of *Bacillus* spores—including *B. anthracis*—and vegetative bacteria at the species level. ***Although there is precedent for analyzing Bacillus spores by CE in the literature, the separation of different Bacillus spore species—and in particular, B. anthracis—is currently unreported.*** Fiber coupled Incoherent Broad-Band Cavity Enhanced Absorption Spectroscopy (IBB-CEAS) has been shown to be a sensitive technique for absorption measurements of NIR absorbing compounds. ***To our knowledge, this work represents the highest sensitivity reported with respect to detection of absorbers in nanoliter samples.*** This detection method has broad applications for sensitive detection of aqueous solutions; however, for particulate samples, a less invasive capillary-fiber interface needs to be developed. For scattering particles, a single pass configuration has been developed for simultaneous scattering/transmission loss measurements which has potential for discrimination based on scattering/transmission ratios as well as peak widths. Potential areas for follow-on development include integrating multiple wavelengths into a single fiber. This would expand the capabilities of both the single pass and cavity enhanced detection schemes for single particle counters, and HPLC detectors (or similar).

For the identification of aerosolized biological agents, this detection approach meets several desired performance parameters for rapid identifier systems: detection in less than 5 minutes, species-level discrimination for *Bacillus* spores including *B. anthracis*, low reagent use and operating costs, compact size (<1ft^3), and detection of 10^4-10^7 organisms/mL sensitivity. A key issue still to be resolved to realize this methodology as a viable fieldable detector is improving the capillary-fiber junction to eliminate particle clogging, and enabling cavity-enhanced detection of particles. Single spore detection with the single-pass system is just at the noise level of the system; because the CEAS technique increases signal (10-fold) but not system noise, it is expected that single spore detection would be easily obtainable. Additional issues include better understanding and reproducibility of spores in the presence of vegetative cells, and implementing physical controls to eliminate particles originating not from the sample.

[This page left intentionally blank]

REFERENCES

1. L. Kremser, D. Blaas and E. Kenndler, "Capillary electrophoresis of biological particles: viruses, bacteria and eukaryotic cells," review, *Electrophoresis* **25**, 2282-2291 (2004).
2. Driks, "Bacillus subtilis spore coat," Microbiology and Molecular Biology Reviews, Mar. 1999, pp. 1-20.
3. S. Mesnage, E. Tosi-Couture, P. Gounon, M. Mock, A. Fouet, "The capsule and S-layer : Two independent and yet compatible macromolecular structures in Bacillus anthracis," *J. Bacteriol.*, **180**, 52-58 (1998).
4. N. Foster, S. Thompson, N. Valentine, J. Amonette, T. Johnson, "Identification of sporulated and vegetative bacteria using statistical analysis of fourier transform mid-infrared transmission data," *Applied Spectroscopy*, 58, 203- 211 (2004).
5. K. Bechtel, R. Zare, A. Kachanov, S. Sanders, B Paldus, "Moving beyond traditional UV-visible absorption detection: Cavity ring-down spectroscopy for HPLC," *Anal. Chem.* **77**, 1177-1182 (2005).
6. L. van der Sneppen, A. Wiskerke, F. Ariese, C. Gooijer, W. Ubachs, "Improving the sensitivity of HPLC absorption detection by cavity ring-down spectroscopy in a liquid-only cavity," *Analytica Chimica Acta* **558**, 2-6 (2006).
7. R. Li, H. P. Loock, and R. D. Oleschuk, "Capillary electrophoresis absorption detection using fiber-loop ring-down spectroscopy," Anal Chem, 78(16), 5685-92 (2006).
8. Z. G. Tong, M. Jakubinek, A. Wright et al., "Fiber-loop ring-down spectroscopy: A sensitive absorption technique for small liquid samples," Review of Scientific Instruments, 74(11), 4818-4826 (2003).
9. T. von Lerber, and M. W. Sigrist, "Cavity-ring-down principle for fiber-optic resonators: experimental realization of bending loss and evanescent-field sensing," Appl Opt, 41(18), 3567-75 (2002).
10. M. Andachi, T. Nakayama, M. Kawasaki et al., "Fiber-optic ring-down spectroscopy using a tunable picosecond gain-switched diode laser," Applied Physics B-Lasers and Optics, 88(1), 131-135 (2007).
11. P. Chanclou, C. Kaczmarek, G. Mouzer et al., "Expanded single-mode fiber using graded index multimode fiber," Optical Engineering, 43(7), 1634-1642 (2004).
12. C. P. Tsekrekos, R. W. Smink, B. P. de Hon et al., "Near-field intensity pattern at the output of silica-based graded-index multimode fibers under selective excitation with a single-mode fiber," Optics Express, 15(7), 3656-3664 (2007).
13. Saile, Elke ; Koehler, Theresa M. Applied and Environmental Microbiology (May 2006) Vol.72, iss.5, p.3168-3174,
14. V. VanderNoot, unpublished results, Sandia National Labs, August 2004.
15. P. S. Tuminello, E. T. Arakawa, B. N. Khare, J. M. Wrobel, M. R. Querry, and M. E. Milham, "Optical properties of Bacillus subtilis spores from 0.2 to 2.5 mm," APPLIED OPTICS Vol. 36, No. 13 1 May 1997.

16. Arakawa, ET ; Tuminello, PS ; Khare, BN ; Milham, ME, “Optical properties of Erwinia herbicola bacteria at 0.190-2.50 mu m,” BIOPOLYMERS (2003) Vol.72, iss.5, p.391-398
17. Arakawa, ET ; Tuminello, PS ; Khare, BN ; Milham, ME, “Optical properties of horseradish peroxidase from 0.13 to 2.5 mu m,” BIOSPECTROSCOPY (1997) Vol.3, iss.1, p.73-80
18. C. P. Tsekrekos, M. de Boer, A. Martinez et al., “Temporal stability of a transparent mode group diversity multiplexing link,” Ieee Photonics Technology Letters, 18(21-24), 2484-2486 (2006).
19. Z. Haas, and M. A. Santoro, “A Mode-Filtering Scheme for Improvement of the Bandwidth Distance Product in Multimode Fiber Systems,” Journal of Lightwave Technology, 11(7), 1125-1131 (1993).
20. M. Duser, and P. Bayvel, “2.5Gbit/s transmission over 4.5km of 62.5 mu m multimode fibre using centre launch technique,” Electronics Letters, 36(1), 57-58 (2000).
21. L. Raddatz, I. H. White, D. G. Cunningham et al., “An experimental and theoretical study of the offset launch technique for the enhancement of the bandwidth of multimode fiber links,” Journal of Lightwave Technology, 16(3), 324-331 (1998).
22. W. Lieber, X. S. Yi, N. Nontasut et al., “Differential mode delay (DMD) in graded-index multimode fiber: effect of DMD on bandwidth tuned by restricted launch conditions,” Applied Physics B-Lasers and Optics, 75(4-5), 487-491 (2002).
23. D. S. Venables, T. Gherman, J. Orphal et al., “High sensitivity in situ monitoring of NO3 in an atmospheric simulation chamber using incoherent broadband cavity-enhanced absorption spectroscopy,” Environ Sci Technol, 40(21), 6758-63 (2006).
24. T. Gherman, D. S. Venables, S. Vaughan et al., “Incoherent broadband cavity-enhanced absorption spectroscopy in the near-ultraviolet: application to HONO and NO2,” Environ Sci Technol, 42(3), 890-5 (2008).
25. T. Wu, W. Zhao, W. Chen et al., “Incoherent broadband cavity enhanced absorption spectroscopy for in situ measurements of NO2 with a blue light emitting diode,” Applied Physics B-Lasers and Optics, 94(1), 85-94 (2009).
26. S. Vaughan, T. Gherman, A. A. Ruth et al., “Incoherent broad-band cavity-enhanced absorption spectroscopy of the marine boundary layer species I-2, IO and OIO,” Physical Chemistry Chemical Physics, 10(30), 4471-4477 (2008).
27. S. E. Fiedler, A. Hese, and A. A. Ruth, “Incoherent broad-band cavity-enhanced absorption spectroscopy of liquids,” Review of Scientific Instruments, 76(2), - (2005)
28. Epolin, [Published with written permission], (2009).

[This page left intentionally blank]

Distribution

1	MS9004	Duane Lindner	08120
1	MS9055	Anthony Gomez	08353
1	MS9056	Ray Bambha	08168
1	MS9292	Julie Fruetel	08125
1	MS9292	Victoria VanderNoot	08621
1	MS9292	Ronald Renzi	08125
1	MS9405	Glenn Kubiak	08600
2	MS9018	Central Technical Files	08944
2	MS0899	Technical Library	04536
1	MS0123	D. Chavez, LDRD Office	01011


Sandia National Laboratories